Relation between macroscopic and microscopic activation energies in nonequilibrium surface processing

M. A. Gosálvez* and R. M. Nieminen

Laboratory of Physics, Helsinki University of Technology, 02015 Espoo, Finland

(Received 22 April 2003; published 22 September 2003)

Realistic Monte Carlo simulations show that the apparent macroscopic activation energy is only partially explained by the expected expression for the average over the microscopic activation energies for surface processing. An additional term accounting for the existence of fluctuations in the fractions of particles has to be taken into account. In all cases considered, the additional term can be accurately estimated by *a posteriori* analysis of the temperature dependence of the surface densities. In addition, we demonstrate that the relative contribution of the different competing microscopic processes to the macroscopic activation energy can be accurately obtained during the simulations, allowing for the unambiguous identification of the particular surface species which effectively control the process. As an example of the nonequilibrium open interfaces to which the results apply, the case of wet chemical etching of crystalline silicon is considered. The results can be directly applied to surface growth.

I. INTRODUCTION

During surface growth and chemical etching, the interface is an example of an evolving nonequilibrium open system driven by the environment through the deposition or removal of particles. The moving surface reaches a steady state with a well-defined apparent macroscopic activation energy (obtained from an Arrhenius plot) for the overall growth or etch rate. Since the macroscopic evolution of the surface—its motion, roughness, and morphology—can be modeled by the local dynamics stemming from a reduced set of microscopic activation energies [1,2], it is physically meaningful to expect an analytical or numerical relation between macroscopic and microscopic activation energies.

The problem of understanding how the macroscopic behavior of a system is related to the interplay between the microscopic motion of the interacting particles and the configurational degeneracy of the available microstates is solved in statistical mechanics in terms of a compromise between internal energy and entropy at any temperature. If the system is in thermal equilibrium and its Hamiltonian can be defined, the macroscopic value of an observable is obtained simply as the (ensemble) average of the values taken by the observable over a large number (ideally infinite) of microstates [3]. However, if the system is far from equilibrium—as is typically the case during surface growth and wet chemical etching—it is not always clear how the macroscopic values of the observables can be found from their microscopic counterparts. As an example, the determination of the exact relation between the macroscopic activation energy of the growth/etch rate and the microscopic activation energies of the atomistic processes occurring at the surface turns out to be a nontrivial problem which has been traditionally overlooked and exceedingly simplified.

Typically, as a result of an iterative sequence of local

processes, a self-organized nonequilibrium steady state with well-defined average values for the observables is reached in these open systems (surfaces). Depending on the problem, the local dynamics may not even be related to an underlying Hamiltonian, but to a set of local activation energies which effectively control the formation of transient species between the different microstates. In these cases, the usual techniques of equilibrium statistical dynamics cannot be used to obtain the averages. Furthermore, some observables—such as the total energy—are not well defined. Only the number of particles removed from (incorporated to) the interface and the energy cost of each removal (incorporation) have a meaning and take indeed well-defined macroscopic values. The problem is to unveil the relation between these macroscopic values and the microscopic realizations of the observable.

The purpose of this paper is to describe several one-dimensional and two-dimensional interface systems where the above mentioned unexpected relation between macroscopic and microscopic activation energies is observed in the context of anisotropic wet chemical etching. In particular, it will be shown that the macroscopic activation energy of the etch rate is explained by the sum of two terms. One of them corresponds to the average of the microscopic activation energies, and the other accounts for the existence of fluctuations in the fractions of particles at fixed temperature. As an important side result, it will be demonstrated that the relative weight of the different microscopic processes for the determination of the activation energy can be accurately obtained during the course of *one* simulation, even if the energy contribution of each process may not be easily determined. In our opinion, this is a most important issue, since it allows for the *unambiguous identification* of the particular surface species which effectively control the etching process, allowing a quantitative measure of the relative importance of majority and minority surface sites. The results directly apply to other systems in surface science, in particular to surface growth.

We will consider three types of systems, representing three different levels of modeling of the etching process (Fig. 1). After giving a general overview of the common features

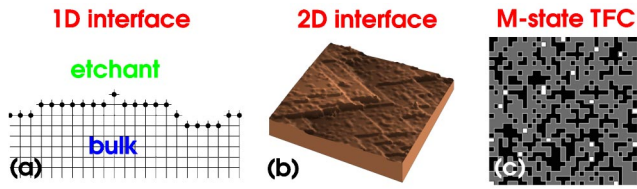*Electronic address: mag@fyslab.hut.fi

FIG. 1. (Color online) Illustration of the interfaces considered in this study: (a) The 1D interface between a 2D square crystal and the environment (an etchant). (b) The 2D interface between crystalline silicon and an etchant [a portion of $\approx 30 \times 30$ nm^2 vicinal Si(111) is shown]. (c) The M-state thermal flipping chessboard (TFC): an analytically solvable 2D model for evolving surfaces.

to the three models in Sec. II and defining in Sec. III the etch rate, the activation energy, and the other quantities required, a simplified two-dimensional exactly solvable surface model is presented in Sec. IV [Fig. 1(c)]. A more realistic model for a two-dimensional solid with a one-dimensional surface is presented in Sec. V [Fig. 1(a)] and a full three-dimensional model for the simulation of anisotropic wet chemical etching of silicon is considered in Sec. VI [Fig. 1(b)]. Finally, we draw our conclusions in Sec. VII.

II. OVERVIEW OF THE MODELS

In this study we consider one-dimensional (1D) and 2D open moving interfaces ("surfaces" embedded in 2D and 3D environments, see Fig. 1) for use in the modeling and understanding of anisotropic wet chemical etching. We present here the general common features to these interfaces.

At any time, the interface is composed of N (not necessarily constant) particles (labeled as $i = 1, 2, \ldots, N$) with removal probabilities

$$p_i = p_{0i} e^{-E_i / k_B T}, \quad (1)$$

where T is the temperature, k_B is the Boltzmann constant, E_i is the microscopic activation energy for the removal from site i, and p_{0i} is a prefactor. Each of the N atoms currently in the surface belongs to one of M different types of sites (also referred to as particle/atom types, labeled as $\alpha = 1, 2, \ldots, M$). All sites of type α share the same prefactor $p_{0\alpha}$ but may have different activation energies.

The reason for choosing this Arrhenius form for the microscopic removal probabilities p_i lies in the experimental fact that the macroscopic etch rate typically follows an Arrhenius dependence on temperature [4,5]. This choice precisely guarantees the macroscopic Arrhenius behavior in the limiting case that the surface is made of only one type of particle. For more types of particles, it is not mathematically guaranteed that a combination of microscopic Arrhenius dependencies will lead to a global Arrhenius behavior. However, if the etching process is controlled by only a few types of particles (perhaps only one), then this choice is expected to provide the correct macroscopic dependence. As will be shown by means of the simulations reported in this work, this assumption typically performs well even for the case when more than one surface species control the etching process.

The dynamics of the surface consists of random removals of sites according to the probabilities p_i. In principle, the microscopic activation energies E_i may be considered as parameters that can be varied at will. However, in the most realistic of the models presented here (Sec. VI), the activation energies are obtained from a local energy function that considers the geometry of the neighborhood, the number of bonds that need to be broken, and the interactions between the surface terminating species, OH and H. In any case, the local activation energies E_i can be thought to effectively control the formation of transient species between the microstates of the surface before and after the removal. In this way, the evolution of the system in these models is not associated to any global energy function or Hamiltonian for the whole system (which would include the surface, the etchant, the bulk, and the species in solution formed as products of the reaction). This does not mean that such a function would not exist. However, it can be anticipated that the form of that function will be very complex and, before it is resolved, we must content ourselves with simplified approaches, such as the local dynamics used in this study. Accordingly, the macroscopic evolution of the surface can be obtained using a Monte Carlo scheme which randomly chooses surface sites and decides whether they are removed or not according to the probabilities p_i, such as that in Ref. [6].

During the time evolution, the state of the surface is characterized by the current numbers of particles of each type $\{N_\alpha\}_{\alpha=1}^M$, or, equivalently, by the current fractions $\{f_\alpha = N_\alpha / N\}_{\alpha=1}^M$. Actually, only $M - 1$ of the $\{f_\alpha\}_{\alpha=1}^M$ variables are required to describe the system, since $\Sigma_\alpha f_\alpha = 1$. For fixed values of the parameters, $\{p_{0\alpha}; E_\alpha\}_{\alpha=1}^M$, and as a result of the iterative sequence of local processes, the surface reaches a self-defined steady state independent of the initial state and characterized by well-defined average values $\{\langle f_\alpha \rangle\}_{\alpha=1}^{M-1}$.

III. ETCH RATE AND ACTIVATION ENERGY

A. Etch rate

The etch rate is defined as the distance traveled by the moving surface per unit time. When the etching process has reached the steady state, the etch rate is simply the ratio of the distance traveled by the center of mass (c.m.) of the surface $\Delta Z_{\text{c.m.}}$ to the period of time elapsed Δt: $R = \Delta Z_{\text{c.m.}} / \Delta t$. During a simulation, $\Delta Z_{\text{c.m.}}$ can be determined as the sum of all individual shifts $(\Delta Z_{\text{c.m.}})_i$ of the surface following each *successful event* (S), i.e., the sum over all successful particle removals $i \in \{S\}$ occurring during Δt,

$$R = \frac{\Delta Z_{\text{c.m.}}}{\Delta t} = \frac{1}{\Delta t} \sum_{i \in \{S\}} (\Delta Z_{\text{c.m.}})_i. \quad (2)$$

Although $(\Delta Z_{\text{c.m.}})_i$ is typically positive, occasionally it may be negative if the removal of site i involves a reduction in the total number of surface sites. In particular, certain site types

of the most realistic of our models for wet chemical etching (e.g., the trihydrides, see Sec. VI) typically contribute to the motion of the c.m. with a negative shift on average. Alternatively, we may consider the sum over *all events* ($i \in \{A\}$), independently of whether or not the event is a successful removal,

$$R = \frac{\Delta Z_{\text{c.m.}}}{\Delta t} = \frac{1}{\Delta t} \sum_{i \in \{A\}} (\Delta Z_{\text{c.m.}})_i p_i. \tag{3}$$

Here p_i is the removal probability of surface atom i, as given by Eq. (1). Note that the (positive/negative) shift of the c.m. of the surface due to the removal of atom i, $(\Delta Z_{\text{c.m.}})_i$, may be calculated independently of whether the atom is removed or not. In principle, Eqs. (2) and (3) give statistically identical results for very long times Δt. In practice, Eq. (3) provides a more robust estimation (better statistics) of the etch rate as it provides averages over *all* events while Eq. (2) averages over only a fraction of them.

Equation (3) suggests that the etch rate is composed of two factors: one purely geometrical (the c.m. shifts) and one purely numerical (the number of removed particles). Indeed, the etch rate R is proportional to the average number of surface atoms removed from the surface per unit time $\langle \dot{N}^{\uparrow} \rangle$,

$$R = \frac{\Delta Z_{\text{c.m.}}}{\Delta t} = \Delta Z \langle \dot{N}^{\uparrow} \rangle, \tag{4}$$

and the proportionality constant ΔZ is precisely a measure of the average shift in the c.m. of the surface per removed atom. ΔZ is an exclusively geometrical feature of the etch rate. In particular, it is independent of temperature. Although ΔZ may take different values for different surface orientations, ΔZ does not depend on temperature for a fixed orientation. In this way, the temperature dependences of R and $\langle \dot{N}^{\uparrow} \rangle$ are the same. This is an important observation because the appearance of negative c.m. shifts $(\Delta Z_{\text{c.m.}})_i$ may affect the interpretation of the relative importance (weight) of the different particle types for the calculation of an average. Actually, the interpretation becomes meaningless if some of the weights are negative. However, the use of $\langle \dot{N}^{\uparrow} \rangle$ is free of these artifacts and allows unambiguous interpretation, as shown in this study.

There are three alternative ways to determine the rate of removal of particles $\langle \dot{N}^{\uparrow} \rangle$ during the simulation.

(i) As in the case of the etch rate R, $\langle \dot{N}^{\uparrow} \rangle$ can be determined during the simulation using only *successful events*, $\langle \dot{N}^{\uparrow} \rangle = (1/\Delta t) \sum_{i \in \{S\}} 1$, or, alternatively, using *all events*,

$$\langle \dot{N}^{\uparrow} \rangle = \frac{1}{\Delta t} \sum_{i \in \{A\}} p_i. \tag{5}$$

Note that the average of the number of surface atoms N (not a constant) can be written similarly as $\langle N \rangle = (1/\Delta t) \sum_{i \in \{A\}} 1$.

(ii) The rate of removal of particles $\langle \dot{N}^{\uparrow} \rangle$ can be written in terms of a sum over the different types of surface sites $\alpha = 1, 2, \ldots, M$,

$$\langle \dot{N}^{\uparrow} \rangle = \sum_{\alpha} \langle N_{\alpha} \rangle \langle p_{\alpha} \rangle, \tag{6}$$

where $\langle p_{\alpha} \rangle$ is the average probability of removal of a surface site of type α,

$$\langle p_{\alpha} \rangle = \frac{\sum_{i \in \alpha} p_i}{\sum_{i \in \alpha} 1}, \tag{7}$$

("$i \in \alpha$" stands for the sum over all events concerning the sites of type α) and $\langle N_{\alpha} \rangle$ is the average number of sites of type α,

$$\langle N_{\alpha} \rangle = \frac{1}{\Delta t} \sum_{i \in \alpha} 1. \tag{8}$$

Note that $\langle N_{\alpha} \rangle \langle p_{\alpha} \rangle$ is the average number of particles of type α that are removed per unit time, denoted as $\langle \dot{N}_{\alpha}^{\uparrow} \rangle$. Thus Eq. (6) is just the sum of the removed particles over all particle types, $\langle \dot{N}^{\uparrow} \rangle = \Sigma_{\alpha} \langle \dot{N}_{\alpha}^{\uparrow} \rangle$.

(iii) The rate of removal of particles $\langle \dot{N}^{\uparrow} \rangle$ may also be expressed in terms of the *average fraction of particles removed per unit time* $\langle \dot{f}^{\uparrow} \rangle$,

$$\langle \dot{N}^{\uparrow} \rangle = \langle N \rangle \langle \dot{f}^{\uparrow} \rangle = \langle N \rangle \sum_{\alpha} \langle f_{\alpha} \rangle \langle p_{\alpha} \rangle. \tag{9}$$

Here we have defined $\langle f_{\alpha} \rangle$ as the *average fraction of particles of type α*,

$$\langle f_{\alpha} \rangle = \frac{\langle N_{\alpha} \rangle}{\langle N \rangle}. \tag{10}$$

As done for interpreting Eq. (6), we can think of the last term in Eq. (9) as a sum over the fractions of particles of each type that are removed per unit time $[\langle \dot{f}_{\alpha}^{\uparrow} \rangle = \langle f_{\alpha} \rangle \langle p_{\alpha} \rangle]$: $\langle \dot{f}^{\uparrow} \rangle = \Sigma_{\alpha} \langle \dot{f}_{\alpha}^{\uparrow} \rangle$.

B. Activation energy

In relation to the etch rate R, the activation energy E_a is, by definition, the slope of the curve $R = R(\beta)$ in an Arrhenius plot, where β is the inverse temperature $\beta = 1/k_B T$,

$$E_a = -\frac{\partial \ln R}{\partial \beta} = -\frac{1}{R} \frac{\partial R}{\partial \beta}. \tag{11}$$

Very often, this curve is a straight line for wide ranges of β and the activation energy is thus a constant. However, it is worth to keep in mind that, in principle, Eq. (11) allows E_a to be any function of β.

As discussed in the context of Eq. (4), the geometrical factor ΔZ is independent of the temperature. Thus the activation energy may be written as the logarithmic derivative of the rate of removal of particles,

$$E_a = -\frac{\partial \ln\langle \dot{N}^\uparrow \rangle}{\partial \beta}. \qquad (12)$$

Note that in principle, we have three alternative equivalent expressions for the rate of removal of particles $\langle \dot{N}^\uparrow \rangle$ [namely, Eqs. (5), (6), and (9)]. Although all three expressions provide the same values for $\langle \dot{N}^\uparrow \rangle$ in the simulations, the final expression for the activation energy is found to depend on the choice. If we consider Eq. (9) and recognize that $\langle N \rangle$, $\langle f_\alpha \rangle$, and $\langle p_\alpha \rangle$ may be functions of the temperature, the derivative in Eq. (12) can be expressed as the sum of three terms,

$$E_a^{(N,f,p)} = E_{\langle N \rangle} + E_a^{(f)} + E_a^{(p)}$$

$$= E_{\langle N \rangle} + \sum_\alpha \langle w_\alpha^\uparrow \rangle E_{\langle f_\alpha \rangle} + \sum_\alpha \langle w_\alpha^\uparrow \rangle E_{\langle p_\alpha \rangle}, \quad (13)$$

where

$$E_{\langle X \rangle} = -\frac{\partial \ln\langle X \rangle}{\partial \beta}, \quad X = N, \ f_\alpha, \ p_\alpha \qquad (14)$$

and $\langle w_\alpha^\uparrow \rangle$ is the *average normalized fraction of removed particles of type* α:

$$\langle w_\alpha^\uparrow \rangle = \frac{\langle \dot{f}_\alpha^\uparrow \rangle}{\sum_\alpha \langle \dot{f}_\alpha^\uparrow \rangle} = \frac{\langle f_\alpha \rangle \langle p_\alpha \rangle}{\sum_\alpha \langle f_\alpha \rangle \langle p_\alpha \rangle}. \qquad (15)$$

However, the use of Eq. (6) as an alternative for $\langle \dot{N}^\uparrow \rangle$ in Eq. (12) results in the last two terms:

$$E_a^{(f,p)} = E_a^{(f)} + E_a^{(p)} = \sum_\alpha \langle w_\alpha^\uparrow \rangle E_{\langle f_\alpha \rangle} + \sum_\alpha \langle w_\alpha^\uparrow \rangle E_{\langle p_\alpha \rangle} , \qquad (16)$$

and the use of Eq. (5) results in the last term only:

$$E_a^{(p)} = \frac{\sum\limits_{i \in \{A\}} p_i E_i}{\sum\limits_{i \in \{A\}} p_i} \qquad (17a)$$

$$= \frac{\sum\limits_\alpha \langle f_\alpha \rangle \langle p_\alpha \rangle E_{\langle p_\alpha \rangle}}{\sum\limits_\alpha \langle f_\alpha \rangle \langle p_\alpha \rangle} \qquad (17b)$$

$$= \sum_\alpha \langle w_\alpha^\uparrow \rangle E_{\langle p_\alpha \rangle}. \qquad (17c)$$

Intuitively, in an initial approach to the determination of E_a, one would expect Eq. (17) [in either form (17a), (17b), or (17c)] to be the correct expression [7]. For instance, in either form (17b) or (17c), it represents the sum (over all species) of the average amount of particles leaving the surface ($\langle w_\alpha^\uparrow \rangle$)

multiplied by the average removal energy cost ($E_{\langle p_\alpha \rangle}$), and in form (17a) it has the typical form of an ensemble average. However, this turns out to be a simplified approach. The previous intuitive reasoning does not take into account the fact that the fractions of particles $\{f_\alpha\}_{\alpha=1}^M$ are functions of temperature. Due to the normalization condition $\Sigma_\alpha f_\alpha = 1$, the fluctuations in the surface fractions at fixed temperature are asymmetric about the average values (Sec. IV C 2), a phenomenon that is macroscopically observed as a preferred direction of change for each of the surface fractions when the temperature is changed. As an example, if $M = 2$, one of the surface fractions increases with temperature while the other decreases. This type of variations in $\langle f_\alpha \rangle$ with temperature is considered in Eqs. (13) and (16) through the terms $E_{\langle f_\alpha \rangle} \neq 0$.

Similarly, one would initially expect $\langle N \rangle$ to change (increase) with temperature. However, this can only happen if the formation of overhangs on the surface is very frequent. On the other hand, for conditions producing single-valued surfaces, which is the case in wet chemical etching, $\langle N \rangle$ does not vary with temperature. Thus, for the purpose of modeling wet chemical etching, $\langle N \rangle$ is independent of the temperature and the use of Eq. (16) instead of Eq. (13) is justified.

Equation (16) is the central result of the present study. By determining the temperature dependence of the removal probabilities $\langle p_\alpha \rangle$ and the surface fractions $\langle f_\alpha \rangle$, it will be shown that the two contributions $E_a^{(p)} + E_a^{(f)}$ accurately describe the macroscopic activation energy of the etch rate. In particular, it will be shown that, in the worst case, $E_a^{(p)}$ and $E_a^{(f)}$ can be accurately estimated in a *a posteriori* analysis of the temperature dependence of the removal probabilities and surface fractions, respectively. An additional interesting feature of Eq. (16) is that the relative weight of each particle type for the determination of the macroscopic activation energy is given by the average normalized fractions of removed particles $\langle w_\alpha^\uparrow \rangle$, which can be easily computed at any temperature during each simulation. As we will see, this will enable an estimation of the relative importance of the different species in the etching process. In particular, it will be shown that the relative contributions ϵ_α of the different atom types to the total macroscopic activation energy, defined from Eq. (16) as

$$\epsilon_\alpha = \frac{\langle w_\alpha^\uparrow \rangle (E_{\langle f_\alpha \rangle} + E_{\langle p_\alpha \rangle})}{\sum\limits_\alpha \langle w_\alpha^\uparrow \rangle (E_{\langle f_\alpha \rangle} + E_{\langle p_\alpha \rangle})}, \qquad (18)$$

are described approximately by $\langle w_\alpha^\uparrow \rangle$ in all models considered, even exactly in one particular model (Sec. IV).

Let us stress the fact that the activation energies $E_{\langle f_\alpha \rangle}$ in Eq. (16) correspond to fluctuations in the numbers of particles N_α at each temperature. To see this, note first that, as a result of the temperature independence of $\langle N \rangle$, we have

$$E_{\langle f_\alpha \rangle} = -\frac{1}{\langle f_\alpha \rangle} \frac{\partial \langle f_\alpha \rangle}{\partial \beta}$$

$$= -\frac{1}{\langle N \rangle \langle f_\alpha \rangle} \frac{\partial (\langle N \rangle \langle f_\alpha \rangle)}{\partial \beta}$$

$$= -\frac{1}{\langle N_\alpha \rangle} \frac{\partial \langle N_\alpha \rangle}{\partial \beta}. \qquad (19)$$

Thus, in order to determine $E_{\langle f_\alpha \rangle}$ it will be sufficient to find an expression for $\partial \langle N_\alpha \rangle / \partial \beta$. In order to do so, we may consider the expression for the fluctuations in the numbers of particles $\langle (\delta N_\alpha)^2 \rangle \equiv \langle N_\alpha^2 \rangle - \langle N_\alpha \rangle^2$ in the grand canonical ensemble for open systems,

$$\langle N_\alpha^2 \rangle - \langle N_\alpha \rangle^2 = \frac{\partial \langle N_\alpha \rangle}{\partial (\beta \mu_\alpha)}, \qquad (20)$$

where μ_α is the chemical potential of the species α. This leads to the following expression for $\partial \langle N_\alpha \rangle / \partial \beta$:

$$\frac{\partial \langle N_\alpha \rangle}{\partial \beta} = (\langle N_\alpha^2 \rangle - \langle N_\alpha \rangle^2) \left(\mu_\alpha + \beta \frac{\partial \mu_\alpha}{\partial \beta} \right). \qquad (21)$$

Thus, Eqs. (19) and (21) formally demonstrate that the activation energies $E_{\langle f_\alpha \rangle}$ are directly related to the fluctuations in the numbers of particles N_α. Unfortunately, it is not clear how the chemical potentials $\mu_\alpha = \partial E / \partial N_\alpha$ can be determined, since the total energy E has not been defined.

The previous interpretation of the term $E_a^{(f)} = \Sigma_\alpha \langle w_\alpha^\uparrow \rangle E_{\langle f_\alpha \rangle}$ as originating from the fluctuations in the numbers of particles N_α illustrates the fact that, as long as the explicit expression for the dependence of $\langle f_\alpha \rangle$ on temperature is not available (or, otherwise, a method to determine the chemical potentials is devised), the determination of the activation energies $E_{\langle f_\alpha \rangle}$ can be done only *a posteriori* by using the simulated data for $\langle f_\alpha \rangle$ at different temperatures. This is precisely the approach taken in the present work in order to understand how the macroscopic activation energy of the etch rate takes a particular value. Incidentally, there exists a nontrivial meaningful model of wet chemical etching for which $E_{\langle f_\alpha \rangle}$ can be calculated analytically. This will be the subject of Sec. IV.

IV. THERMAL FLIPPING CHESSBOARD (TFC)

A. The *M*-particle TFC model

Consider a two-dimensional system composed of two types of sites ("white" and "black" or, equivalently, "1" and "0") in which the white (black) sites have a probability $p_1 = p_{01} e^{-E_1 / k_B T}$ ($p_0 = p_{00} e^{-E_0 / k_B T}$) to be removed from the system, independently of the state of their neighborhood. The removal of a white (black) site leads to the appearance of a black (white) site with probability $\pi_{1 \to 0}$ ($\pi_{0 \to 1}$) and of a white (black) site with probability $\pi_{1 \to 1}$ ($\pi_{0 \to 0}$). The transition matrix $\mathbf{\Pi} = (\pi_{\alpha \beta}) \equiv (\pi_{\alpha \to \beta})$ characterizes the probability of any conversion between the two species. Since every removed site is always replaced by another site (which can be of either type) the transition matrix $\mathbf{\Pi}$ satisfies the following normalization conditions:

$$\pi_{00} + \pi_{01} = 1, \qquad \pi_{10} + \pi_{11} = 1. \qquad (22)$$

The local dynamics of the system consists of random removals of white and black sites with probabilities p_1 and p_0, leading to the appearance of white or black sites according to the probabilities $\pi_{\alpha \beta}$. The macroscopic evolution of the system is obtained as indicated in Sec. II. The state of the system is characterized by, e.g., f_1 (as f_0 is obtained from $f_0 + f_1 = 1$) and the total number of sites N is constant. The system is purely two dimensional and there are no height changes associated to the site removals. In consequence, the etch rate in this model can only be defined as the rate of removal of particles $\langle \dot{N}^\uparrow \rangle$. The equivalent fractional measure $\langle \dot{f}^\uparrow \rangle$ will be used.

The important feature of the current model is that it offers the possibility to study the relation between macroscopic and microscopic activation energies without the additional difficulties involved in more realistic models of wet chemical etching. The interesting feature of the model resides in the use of the temperature T and not in the existence of two states. In fact, the number of states may become arbitrarily large (say M) without further complications. We will refer to the proposed M-particle model as the *thermal flipping chessboard*. Figure 1(c) shows a snapshot of the $M = 3$ TFC model.

Note that the two-state TFC model ($M = 2$) can be mapped to the 2D Ising model [8], although no interactions between the neighbors have been defined through a Hamiltonian and, in general, the transitions between the two states are partial (as implied by a general transition matrix). The relation between the two models becomes clearer in the particular case that the transition matrix is chosen as

$$\begin{pmatrix} \pi_{00} & \pi_{01} \\ \pi_{10} & \pi_{11} \end{pmatrix} = \begin{pmatrix} 0 & 1 \\ 1 & 0 \end{pmatrix}, \qquad (23)$$

in which case every white site that is removed is replaced by a black site, and the reverse. In principle, the M-particle TFC can be similarly mapped to the q-state Potts model [9].

The TFC model contains the basic ingredient for the simulation of chemical etching, namely, that the removal of one surface site produces the incorporation of new sites into the surface and/or a transformation of the site type of the already existing neighboring surface sites. This essential feature is incorporated in the model by the use of the transition matrix $\mathbf{\Pi}$. The TFC model is convenient for two reasons: first, because the total number of particles N in the system is fixed; second, because there are no geometrical changes involved in the site-type transformations. These two features differ from the typical case found in more realistic models of chemical etching (Secs. V and VI) and will allow us to demonstrate that the deviations in the determination of the macroscopic activation energy (occurring both in this and the more realistic models) are neither related to fluctuations in the *total* number of particles N nor to complicated geometrical effects.

In the TFC model, the transition matrix $(\pi_{\alpha\beta})$ is a parameter, independent of other variables such as the removal probabilities p_α and the temperature T. This turns out to be a useful difference with respect to the more realistic systems, in which the transition matrix depends on the removal probabilities, the temperature, and the underlying geometry of the bulk structure. In fact, the independence of $\mathbf{\Pi}$ from temperature allows one to solve analytically the TFC model exactly for any number M of particle types. This makes the TFC systems ideal for testing and judging the goodness of our approach for the (*a posteriori*) determination of the contribution $E_a^{(f)}$ in Eq. (16) in more realistic models of wet etching.

B. Analytical solution of the *M*-particle TFC model

Consider the M-particle TFC model introduced in the preceding section. At any instant, the rate of change in the fraction of particles of type α is given by the master equation

$$\frac{\partial f_\alpha}{\partial t} = -p_\alpha f_\alpha + \sum_{\beta=1}^{M} \pi_{\beta\alpha} p_\beta f_\beta \quad (\forall\ \alpha=1,2,\ldots,M),$$

(24)

where $-p_\alpha f_\alpha$ is the number of particles of type α being removed and $\Sigma_{\beta=1}^M \pi_{\beta\alpha} p_\beta f_\beta$ corresponds to the number of α particles being created due to the removal of all other types. Here $\mathbf{\Pi} = (\pi_{\alpha\beta}) \equiv (\pi_{\alpha\to\beta})$ is the transition matrix whose element $\pi_{\beta\alpha} = \pi_{\beta\to\alpha}$ describes the probability that a site of type α will be created following the removal of a site of type β. Since the removal of one particle always leads to the appearance of another particle, the transition matrix satisfies the normalization condition

$$\sum_{\beta=1}^{M} \pi_{\alpha\beta} = 1 \quad (\forall\ \alpha=1,2,\ldots,M).$$

(25)

We are interested in finding the values of f_α that are solutions of the steady state of Eq. (24) ($\partial f_\alpha/\partial t = 0$) and simultaneously satisfy the restriction:

$$\sum_{\alpha=1}^{M} f_\alpha = 1.$$

(26)

In the steady state, Eq. (24) can be written as

$$\underbrace{\begin{pmatrix} \pi_{11}-1 & \pi_{21} & \pi_{31} & \cdots & \pi_{M1} \\ \pi_{12} & \pi_{22}-1 & \pi_{32} & \cdots & \pi_{M2} \\ \pi_{13} & \pi_{23} & \pi_{33}-1 & \cdots & \pi_{M3} \\ \vdots & \vdots & \vdots & \ddots & \vdots \\ \pi_{1M} & \pi_{2M} & \pi_{3M} & \cdots & \pi_{MM}-1 \end{pmatrix}}_{\mathbf{A}=\mathbf{\Pi}^\dagger-\mathbf{I}} \underbrace{\begin{pmatrix} p_1 f_1 \\ p_2 f_2 \\ p_3 f_3 \\ \vdots \\ p_M f_M \end{pmatrix}}_{\mathbf{g}} = \underbrace{\begin{pmatrix} 0 \\ 0 \\ 0 \\ \vdots \\ 0 \end{pmatrix}}_{\mathbf{0}},$$

(27)

where $\mathbf{\Pi}^\dagger$ is the transpose of $\mathbf{\Pi}$ and $\mathbf{I}$ is the identity matrix. Writing $\pi_{\alpha\alpha}-1 = -\Sigma_{\beta\neq\alpha}\pi_{\alpha\beta}$ from Eq. (25) shows that $\det(\mathbf{A})=0$. Thus, one of the M equations is redundant (e.g., the last one) and may be substituted by Eq. (26), as in

$$\begin{pmatrix} (\pi_{11}-1)p_1 & \pi_{21}p_2 & \pi_{31}p_3 & \cdots & \pi_{M1}p_M \\ \pi_{12}p_1 & (\pi_{22}-1)p_2 & \pi_{32}p_3 & \cdots & \pi_{M2}p_M \\ \pi_{13}p_1 & \pi_{23}p_2 & (\pi_{33}-1)p_3 & \cdots & \pi_{M3}p_M \\ \vdots & \vdots & \vdots & \ddots & \vdots \\ 1 & 1 & 1 & \cdots & 1 \end{pmatrix} \begin{pmatrix} f_1 \\ f_2 \\ f_3 \\ \vdots \\ f_M \end{pmatrix} = \begin{pmatrix} 0 \\ 0 \\ 0 \\ \vdots \\ 1 \end{pmatrix}.$$

(28)

After some algebra, the solution to Eq. (28) is found to be (note $f_\alpha \to \langle f_\alpha\rangle$ and $p_\alpha \to \langle p_\alpha\rangle$)

$$\langle f_\alpha\rangle = \frac{\dfrac{c_\alpha}{\langle p_\alpha\rangle}}{\displaystyle\sum_{\beta=1}^{M} \frac{c_\beta}{\langle p_\beta\rangle}} \quad (\alpha=1,2,\ldots,M),$$

(29)

where

$$c_\alpha = \det(\mathbf{M}_{\alpha\alpha}^{\mathbf{A}})$$

(30)

and $\mathbf{M}_{\alpha\alpha}^{\mathbf{A}}$ is the matrix minor corresponding to element $A_{\alpha\alpha}$ of matrix $\mathbf{A}$. For instance, if $M=3$ one gets

$$c_1 = 1 - \pi_{22} - \pi_{33} + \pi_{22}\pi_{33} - \pi_{23}\pi_{32},$$

(31)

and similar relations for c_2 and c_3.

The eigenvalue-problem form of Eq. (27) suggests an alternative way to solve for the steady-state surface fractions f_α. The idea is to solve first for the eigenvector $\mathbf{g} = (g_1, g_2, \ldots, g_M)$ corresponding to the eigenvalue $\lambda = 1$ of $\mathbf{\Pi}^\dagger$ and to find $\mathbf{f}$ as $(f_1, f_2, \ldots, f_M) = (g_1/p_1, g_2/p_2, \ldots, g_M/p_M)$. This can be done by multi-

plying $\mathbf{\Pi}$ by itself several times until the result does not vary, and taking $(g_1, g_2, \ldots, g_M)$ as any of the rows of the resulting matrix [10]. This procedure is computationally more efficient for the determination of the c_α's (as g_α's) if the number of particle types M is large. The advantage of the approach followed in the derivation of Eq. (29) is that it provides an exact analytical expression for $\langle f_\alpha \rangle$ in terms of the removal probabilities $\langle p_\alpha \rangle$ and the transition matrix $\mathbf{\Pi}$.

The physical meaning of Eq. (29) is intuitively simple as it states that the average number of particles $\langle f_\alpha \rangle$ of type α at the surface is inversely proportional to their removal probability $\langle p_\alpha \rangle$ and proportional to the removal probabilities of the rest species through the normalizing factor $\Sigma_{\beta=1}^M c_\beta / \langle p_\beta \rangle$. Note that, in addition to the steady-state condition for the master equation [Eq. (24)], the derivation of Eq. (29) makes use of very general relations, such as Eqs. (25) and (26). Therefore, it would seem that Eq. (29) is very general and should be valid also for other models of wet chemical etching. This is not the case, as will be shown in Sec. V.

Due to the temperature independence of the coefficients c_α in Eq. (29), an exact expression for the macroscopic activation energy can be obtained for the M-particle TFC model. The independence of c_α from temperature stems from the fact that, according to Eq. (30), the coefficients c_α are completely determined by the transition matrix $\mathbf{\Pi}$, which, being an input parameter in this model, is fixed for all temperatures. Thus the evaluation of $E_{\langle f_\alpha \rangle} = -\partial \ln\langle f_\alpha \rangle / \partial(1/k_B T)$ [using Eq. (29)] for the determination of the macroscopic activation energy according to Eq. (16) becomes straightforward. The result is

$$E_{\langle f_\alpha \rangle} = -E_{\langle p_\alpha \rangle} + \sum_{\beta=1}^M \langle f_\beta \rangle E_{\langle p_\beta \rangle}. \tag{32}$$

Thus, the macroscopic activation energy can be determined by substituting Eq. (32) into Eq. (16) to get

$$E_a = \sum_{\alpha=1}^M \langle f_\alpha \rangle E_{\langle p_\alpha \rangle}. \tag{33}$$

Equation (33) provides a very simple relation between the microscopic energies $E_{\langle p_\alpha \rangle}$ and the macroscopic energy E_a for the M-particle TFC model with temperature-independent transition matrix. The simplicity of this result is surprising. After all, the macroscopic activation energy in the TFC model is literally the "total energy" of the surface. However, this result should not be overinterpreted by expecting the same to be true in other models. In particular, Eq. (33) fails to provide the macroscopic activation energy in the case of temperature-dependent transition matrices, which is the case in more realistic approaches to wet chemical etching. Moreover, it is easily verified that in the TFC model the relative contributions ϵ_α of the different atom types to the total macroscopic activation energy, defined in Eq. (18), take the simple value $\epsilon_\alpha = \langle w_\alpha^\uparrow \rangle$, while the alternative definition from Eq. (33),

$$\tilde{\epsilon}_\alpha = \frac{\langle f_\alpha \rangle E_{\langle p_\alpha \rangle}}{\sum_\alpha \langle f_\alpha \rangle E_{\langle p_\alpha \rangle}}, \tag{34}$$

does not lead to a simplified expression. This suggests that the normalized fractions of removed particles $\langle w_\alpha^\uparrow \rangle$ are a natural measure of the relative importance of the different surface sites for the macroscopic activation energy, as they clearly are (by definition) for the etch rate R itself. Actually, we will see that, although $\epsilon_\alpha \neq \langle w_\alpha^\uparrow \rangle$ in the more realistic models, the two measures take similar values and the normalized fractions $\langle w_\alpha^\uparrow \rangle$ can be used as indicators of relative importance.

C. Results for the TFC model

1. Macroscopic activation energy

We report on results for the TFC model on square regions containing $N = 2500$, $10\,000$, and $40\,000$ sites for two-particle ($M = 2$) and three-particle ($M = 3$) systems. Since the TFC model is analytically solvable for any M (Sec. IV B), the purpose of this section is not to provide numerical proof of the exact results but to illustrate by means of a few examples how the values of the temperature-averaged macroscopic activation energy can be accurately described in *a posteriori* analysis of the results at different temperatures. This will support the analysis made in the more realistic models of wet etching.

For $M = 2$, we consider two examples for the case of the trivial transition matrix given by Eq. (23) (cases A and B) and a third example (case C) for a more general transition matrix, chosen as

$$\mathbf{\Pi} = \begin{pmatrix} 0.25 & 0.75 \\ 0.65 & 0.35 \end{pmatrix}. \tag{35}$$

Two representative examples for the case of different energies [11] ($E_1 = 0.3$ eV, $E_0 = 0.5$ eV) are considered: (A) equal prefactors ($p_{01} = p_{00} = 5 \times 10^3$) and ($B$ and C) different prefactors ($p_{01} = 5 \times 10^3$, $p_{00} = 2 \times 10^6$). For $M = 3$ (case D) the transition matrix $\mathbf{\Pi}$, the microscopic activation energies E_α (in eV), and the prefactors $p_{0\alpha}$ are chosen as follows:

$$\mathbf{\Pi} = \begin{pmatrix} 0.001\,10 & 0.080\,56 & 0.918\,34 \\ 0.029\,37 & 0.472\,02 & 0.498\,61 \\ 0.039\,61 & 0.585\,81 & 0.374\,58 \end{pmatrix},$$

$$\begin{pmatrix} E_1 \\ E_2 \\ E_3 \end{pmatrix} = \begin{pmatrix} 0.0 \\ 0.3 \\ 0.5 \end{pmatrix}, \quad \begin{pmatrix} p_{01} \\ p_{02} \\ p_{03} \end{pmatrix} = \begin{pmatrix} 1.0 \\ 5 \times 10^3 \\ 2 \times 10^6 \end{pmatrix}. \tag{36}$$

This choice of $\mathbf{\Pi}$ corresponds to the transition matrix of a one-dimensional interface with three types of particles at low temperature (Sec. V), whose microscopic activation energies and prefactors are similar to those of Eq. (36) and whose dynamics are dominated by slow etch pit formation followed

TABLE I. Summary of parameters for cases A, B, and C.

	N	p_{01}	p_{00}	$E_1(eV)$	$E_0(eV)$	Π
A	100×100	5×10^3	5×10^3	0.3	0.5	Eq. (23)
B	100×100	5×10^3	2×10^6	0.3	0.5	Eq. (23)
C	50×50	5×10^3	2×10^6	0.3	0.5	Eq. (35)
D^{a}	50×50					

[a] Parameters for case D from Eq. (36).

by fast step propagation. A summary of the choice of parameters for cases A, B, C, and D is given in Table I.

Figure 2(a) shows the rate of removal of particles $\langle \dot{f}^{\uparrow} \rangle$ as a function of temperature for case D as an example of the typical behavior obtained in all cases. The exact curve in the main frame is obtained by plotting $\langle \dot{f}^{\uparrow} \rangle$ from Eq. (9) with $\langle f_\alpha \rangle$ from Eq. (29) and c_α from Eq. (30). In the case of the exact curve for the macroscopic activation energy E_a in the inset, Eq. (33) is used. The agreement between the simulation points and the exact curve (main frame) is very good. Note that the exact curve is slightly bent, illustrating the fact

that the combination of microscopic removal rates (each following the Arrhenius behavior) does not guarantee linear Arrhenius behavior for the global macroscopic rate (Sec. II). As a result, the macroscopic activation energy is not constant but, rather, a (smooth) function of temperature, as shown in the inset. Nevertheless, the assumption of linear macroscopic behavior and constant activation energy is reasonably good as the range of temperatures of interest in wet chemical etching is small. This is shown by the similarity between the slope of the linear fit $E_a^{\text{lin-fit}} \approx 0.44$ eV and the average slope of the exact curve $\langle E_a \rangle \approx 0.42$ eV (inset). Closer results are obtained for cases $A-C$.

Let us now pretend for a moment that the temperature dependence of $\langle f_\alpha \rangle$ is not analytically known *a priori* (as it is the case for the more realistic models of wet etching), so that an exact expression for the macroscopic activation energy [as Eq. (33) for the TFC model] cannot be derived. It is still possible to understand how the macroscopic activation energy (considered as an average over all temperatures, i.e., essentially as the slope of the linear fit) gets its value. The macroscopic activation energy obtained from the linear fit of Fig. 2(a) (and corresponding linear fits for cases $A-C$) is shown in Fig. 3, together with the values for the contribu-
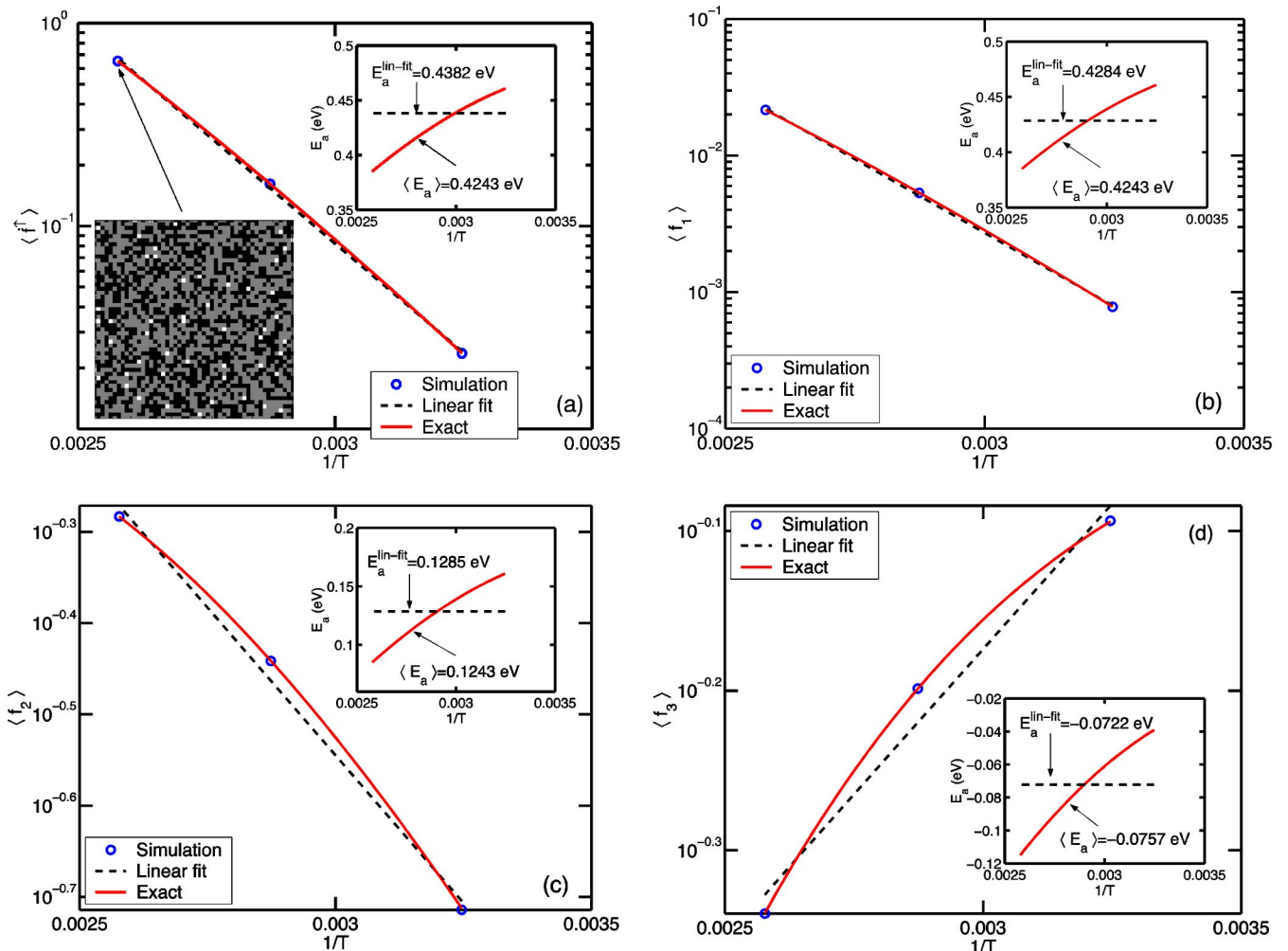

FIG. 2. (Color online) Arrhenius plot of (a) the rate of removal of particles $\langle \dot{f}^{\uparrow} \rangle$ and the surface fractions (b) $\langle f_1 \rangle$, (c) $\langle f_2 \rangle$, and (d) $\langle f_3 \rangle$ for case D.
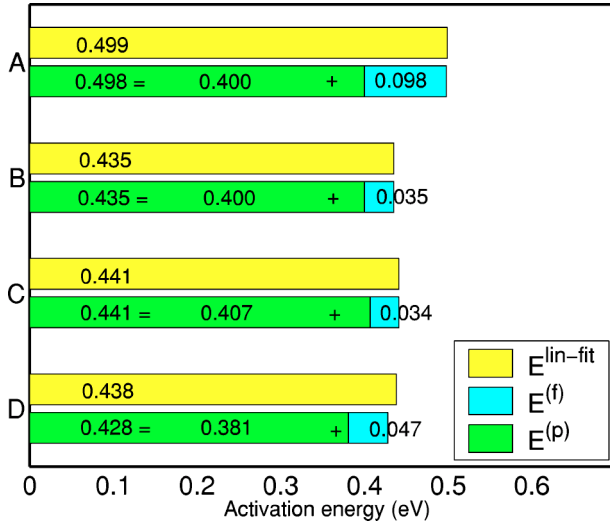
FIG. 3. (Color online) Activation energy $E_a^{\text{lin-fit}}$ explained as the sum $E_a^{(p)} + E_a^{(f)}$ [Eq. (16)] for cases A–D.

tions $E_a^{(p)}$ and $E_a^{(f)}$ [defined through Eq. (16)]. Figure 3 shows that the term $E_a^{(p)}$ alone fails to explain the macroscopic activation energy in all four cases and that the term $E_a^{(p)}$ accurately describes the deviations. The macroscopic activation energy is thus explained as the sum $E_a^{(p)} + E_a^{(f)}$. Note that the value of $E_a^{(p)}$ is computed at each temperature during the simulations [using $E_{\langle p_\alpha \rangle} = E_\alpha$ in Eq. (17) with the weights $\langle w_\alpha^\uparrow \rangle$ given by Eq. (15)] but, since the temperature dependence of $\langle f_\alpha \rangle$ is not known *a priori* (as we are pretending), $E_a^{(f)}$ can "only" be determined *a posteriori* from the temperature analysis of the values obtained in the simulations. This is done in Figs. 2(b)–2(d), where it is shown that linear fits to the simulation results for $\langle f_\alpha \rangle$ can be used to provide approximations to the values of the slopes $E_{\langle f_\alpha \rangle}$. The values quoted in Fig. 3 for $E_a^{(p)}$, $E_a^{(f)}$, and $E_a^{(p)} + E_a^{(f)}$

correspond to the temperature-averaged values over the simulated temperatures.

The previous procedure, although not strictly required for the exactly solvable TFC model, illustrates the method that will be applied in the more realistic models of wet etching in order to describe the temperature-averaged values of the macroscopic activation energies. It shows that the (temperature-averaged) macroscopic activation energy— described approximately by the slope of a linear fit—can be approximated by evaluating the term $E_a^{(f)} = \Sigma_\alpha \langle w_\alpha^\uparrow \rangle E_{\langle f_\alpha \rangle}$ *a posteriori* from the temperature dependence of the surface fractions $\langle f_\alpha \rangle$.

2. Non-Gaussian statistics

As commented in Sec. III B, the fluctuations in the numbers of particles N_α (or, equivalently, in f_α) are expected to be asymmetric about their mean value $\langle f_\alpha \rangle$, due to the constraint $\Sigma_\alpha f_\alpha = 1$ ($0 < f_\alpha < 1$).

As an example of this typical feature, Fig. 4(a) shows the probability density function $P(f_1)$ at three temperatures for case A (Sec. IV C 1). Following Ref. [12], $P(f_1)$ is shown as the quantity $\sigma P(f_1)$ plotted against $(f_1 - \langle f_1 \rangle)/\sigma$ for better comparison of the different probability densities. Here, σ is the standard deviation of the data, $\sigma = [\Sigma P(f_1)(f_1 - \langle f_1 \rangle)^2]^{1/2}$. If $P(f_0)$ were drawn in this figure, a mirror reflection of the shown curves about $(f_1 - \langle f_1 \rangle)/\sigma = 0$ would be obtained.

The main feature of the probability densities is the asymmetry (skewness). Figure 4(a) shows that, as the temperature is decreased, the distribution becomes more skewed and the mean value decreases. Similarly, the skewness of the distribution increases as the system size is decreased [Figure 4(b)], although in this case the mean value does not depend on size. The reason for this increase in skewness with decreasing temperature and decreasing size can be found in the constraint $\Sigma_\alpha f_\alpha = 1$, with $0 < f_\alpha < 1$.
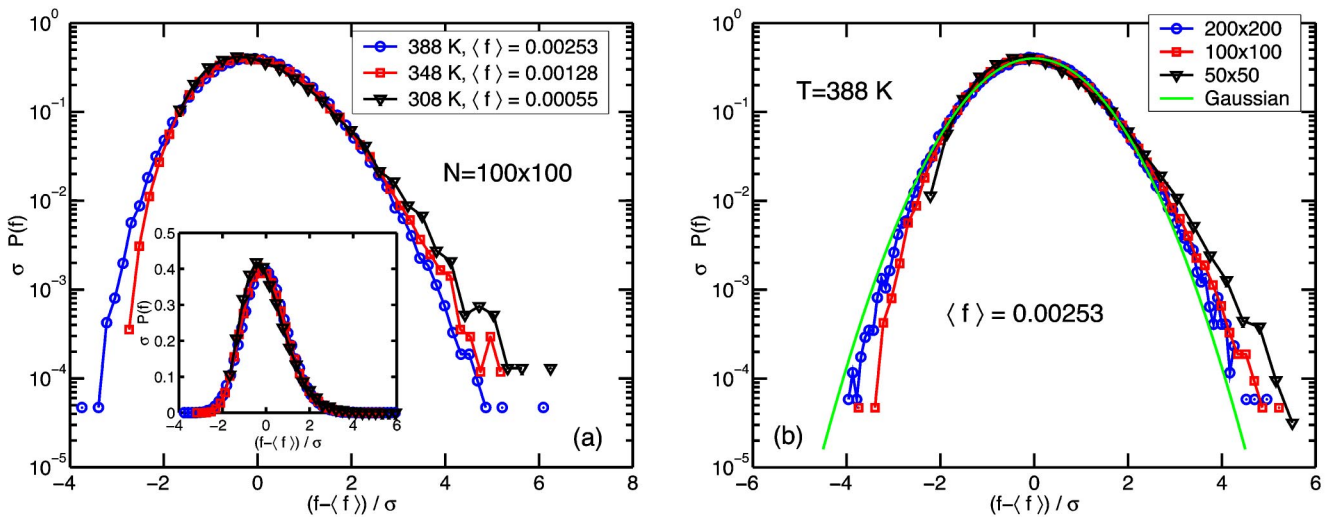

FIG. 4. (Color online) Probability density function $P(f)$ for the fluctuations in the fraction of particles of type 1 ($f \equiv f_1$) for case A: (a) at three different temperatures in logarithmic and natural (inset) scale, and (b) for three system sizes $N = 50 \times 50$, 100×100, 200×200. $\langle f \rangle = 0.002\,53$ for all cases in (b).
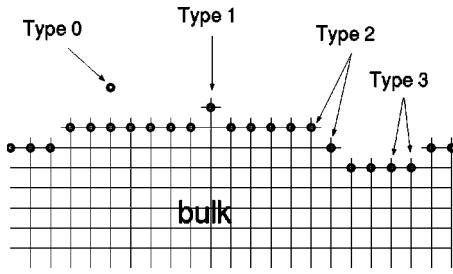
FIG. 5. Schematic representation of the one-dimensional interface showing the four types of atom ($\alpha = 0,1,2,3$) depending on their number of links.

In the case of the variation with temperature, note that the mean values $\langle f_1 \rangle$ and $\langle f_0 \rangle = 1 - \langle f_1 \rangle$ get more separated from each other and, correspondingly, closer to their limiting values (0 and 1, respectively) as the temperature is decreased [legend in Fig. 4(a)]. Since $\langle f_1 \rangle$ cannot become less than zero and $\langle f_0 \rangle$ cannot be larger than 1, the fluctuations are forced to occur more frequently within the region between the two mean values. As a result, the positive tail of $P(f_1)$ grows at the expense of the negative tail, and the reverse occurs for $P(f_0)$.

The increase of skewness with decreasing system size is explained by the inherent discreteness of $\langle f_\alpha \rangle$ in small systems. In Fig. 4(b), where the mean value $\langle f_1 \rangle$ does not depend on size, the average number of particles of type 1 ($\langle N_1 \rangle = N \langle f_1 \rangle$) is about 101 for $N = 200 \times 200$, about 25 for $N = 100 \times 100$, and about 6 for $N = 50 \times 50$. Thus, in absolute terms, the fluctuations of N_1 to the left of $\langle N_1 \rangle$ are more restricted in the smaller systems and, as a result, the smaller systems spend more time at the right of $\langle N_1 \rangle$. In the limit of large system size, the fluctuations become Gaussian, as suggested by Fig. 4(b).

We stress that, even though the distribution of the fluctuations depends on the system size, the average values of all macroscopic quantities (such as, $\langle f_\alpha \rangle$, $\langle w_\alpha^\uparrow \rangle$, $\langle \dot{f}^\uparrow \rangle$ and the macroscopic activation energy E_a) are size independent. In addition to Fig. 4(b), this is supported by the excellent agreement between the exact curves and the simulation results (points) provided in Fig. 2 for $N = 50 \times 50$ (and similar figures for cases $A - C$, not shown).

V. ONE-DIMENSIONAL INTERFACE

A. Description of the 1D model

We turn now to the next level of difficulty in the modeling of wet chemical etching by considering an interface with a self-defined transition-probability matrix. Consider a one-dimensional "surface" between a square lattice (whose nodes represent atoms in the bulk) and the etchant region (represented by the empty nodes of the lattice). The surface is defined as the set of occupied nodes having less than four links to neighboring occupied nodes and, thus, it may contain $M = 3(+1)$ types of surface sites (Fig. 5). The sites having 0 links (type 0) are included for completeness, since overhangs can occur in our simulations. As already commented in Sec. III B, these are rare events for the choice of parameters used to model wet etching and, in practice, they have negligible influence in the behavior of the interface. This explains the previous notation "$M = 3(+1)$" for the number of atom types.

The local dynamics of this system consists of random removals of particles from the surface (with probabilities $p_\alpha = p_{0\alpha} e^{-E_\alpha / k_B T}$, $\alpha = 0,1,2,3$) and a Monte Carlo scheme can be used, as previously, in order to determine the macroscopic evolution of the surface. After each removal, the site type of each neighboring atom needs to be updated. Keeping track of all created/updated site types corresponding to each site removal allows one to obtain the transition matrix $\mathbf{\Pi} = (\pi_{\alpha\beta}) = (\pi_{\alpha \to \beta})$, which describes the probability that a site of type β will be created following the removal of a site of type α. The state of the system is characterized by, e.g., $\{f_1, f_2, f_3\}$, since f_0 is obtained from $\Sigma_\alpha f_\alpha = 1$. The total number of sites N (not constant) fluctuates about the value imposed by the horizontal size of the system. The rate of removal of particles $\langle \dot{f}^\uparrow \rangle$ will be used as a measure of the etch rate $R = \Delta Z \langle N \rangle \langle \dot{f}^\uparrow \rangle$.

B. Results for the 1D model

We consider an interface with linear size $N = 200$ and report on four representative cases of parameter values, as shown in Table II. The choice of parameters in E was made to provide comparison with the TFC model of Sec. IV C 1. The parameters in H result in an atomistically flat surface, characterized by slow etch pitting and fast step propagation. In F, the surface becomes rougher as the rates of etch pitting and step propagation are more similar. Although G also results in an atomistically rough surface, it is included as an anticipation of the more realistic simulations presented in Sec. VI. Based on this example, we will see that the average activation energy associated to an atom type does not correspond to the mean energy if the microscopic activation energy of that atom is uniformly distributed over an interval.

TABLE II. Parameter values for cases E, F, G, and H.

	p_{01}	p_{02}	p_{03}	p_{04}	E_1	E_2	E_3	E_4
E	5×10^3	5×10^3	5×10^3	5×10^3	0.3	0.3	0.5	0.3
F	1.0	5×10^3	5×10^5	1.0	0.0	0.3	0.55	0.0
G	1.0	5×10^3	5×10^5	1.0	0.0–0.1 [a]	0.3–0.5 [a]	0.55–0.85 [a]	0.0
H	1.0	8×10^4	5×10^5	1.0	0.0	0.4	0.75	0.0

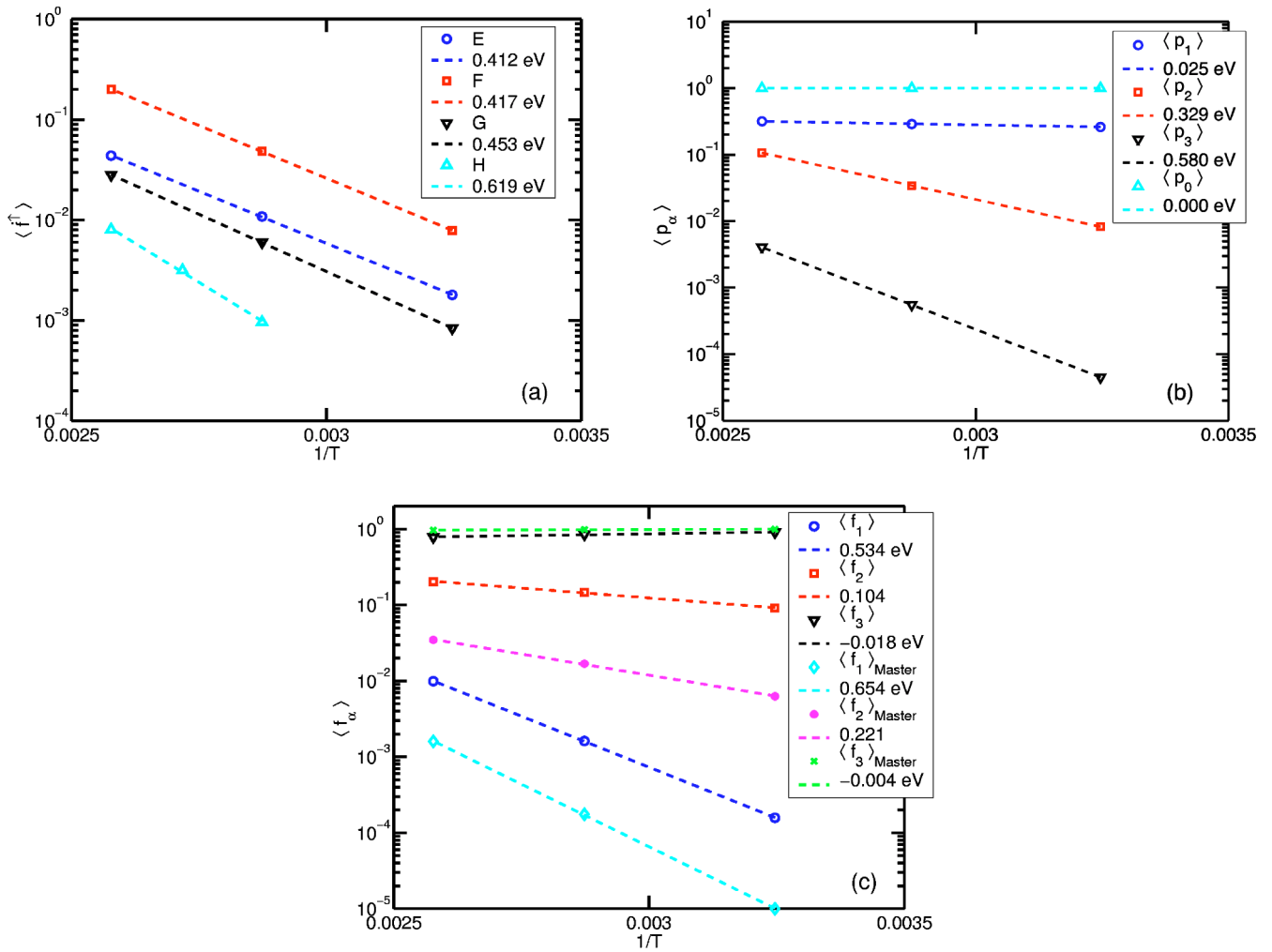[a]Random activation energies are uniformly chosen from the shown interval. Energies are measured in eV.

FIG. 6. (Color online) (a) Rate of removal of particles $\langle \dot{f}^{\uparrow} \rangle$ for cases E, F, G, and H. (b),(c) Determination of the activation energies $E_{\langle p_\alpha \rangle}$ ($\alpha = 0,1,2,3$) and $E_{\langle f_\alpha \rangle}$ ($\alpha = 1,2,3$) for case G. In (c), $\langle f_\alpha \rangle_{\text{master}}$ corresponds to the values calculated using Eq. (29). The case $\alpha = 0$ is not shown as $\langle f_0 \rangle \lesssim 10^{-6}$.
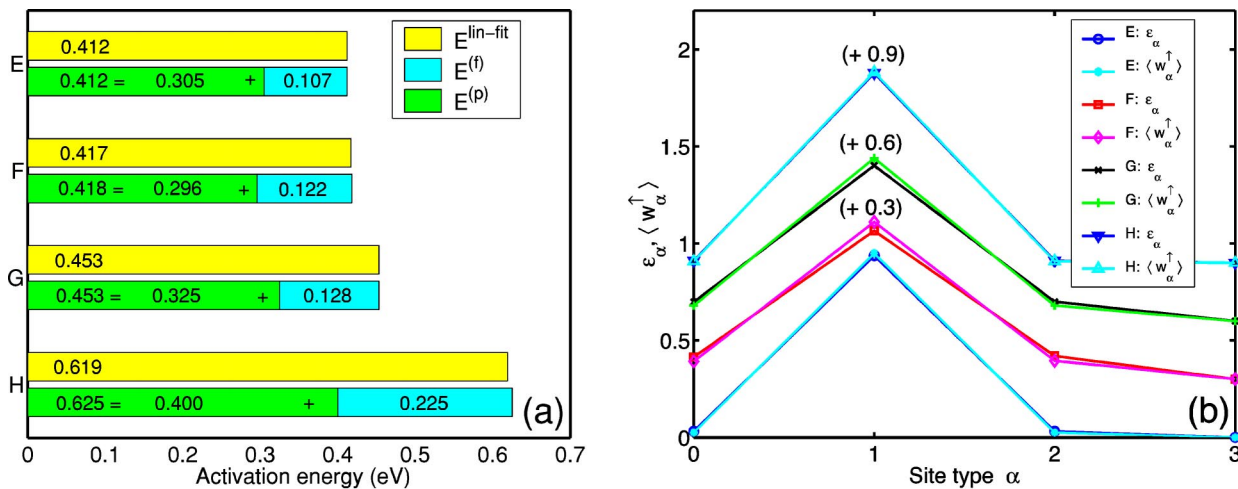

FIG. 7. (Color online) (a) Activation energy $E_a^{\text{lin-fit}}$ explained as the sum $E_a^{(p)} + E_a^{(f)}$ [Eq. (16)] for cases E-H. (b) Relative contributions ϵ_α [Eq. (18)] compared to the normalized fractions $\langle w_\alpha^{\uparrow} \rangle$ [Eq. (15)] for cases E-H. Straight lines are guides for the eyes.

We determine the macroscopic activation energy corresponding to the etch rate from the Arrhenius plot $\ln\langle \dot{f}^\uparrow \rangle$ vs β in Fig. 6(a) and provide an example of the temperature analysis of $\langle p_\alpha \rangle$ and $\langle f_\alpha \rangle$ for case G in Figs. 6(b)–6(c). In all four cases, the macroscopic activation energy ($E_a^{\text{lin-fit}}$) differs from the values provided by $E_a^{(p)}$ [Eq. (17)] and the differences are explained by the fluctuations in the numbers of particles $E_a^{(f)}$. A summary of the results for all four cases is given in Fig. 7(a).

It is interesting to note that, although the activation energies for the microscopic removal probabilities p_i are distributed uniformly in intervals for case G (Table II), according to Fig. 6(b) the average activation energy for each particle type $E_{\langle p_\alpha \rangle}$ does not correspond to the mean value of each energy interval. Actually, the values obtained from the linear fits in Fig. 6(b) are in excellent agreement with those (not shown) obtained during the simulations by using Eq. (17) restricted to the atom type considered (i.e., $i \in \alpha$):

$$E_{\langle p_\alpha \rangle} = \frac{\sum\limits_{i \in \alpha} p_i E_i}{\sum\limits_{i \in \alpha} p_i}. \tag{37}$$

This illustrates the fact that Eq. (17) is physically meaningful when all particles are of the same type (i.e., have the same prefactors, although different activation energies) and there are no fluctuations in the surface fractions. However, if the different activation energies for the same atom type are not distributed uniformly over an energy interval but, rather, form a discrete set of energies, the problem of determining the average activation energy for an atom type becomes formally equivalent to the problem of determining the macroscopic activation energy for the whole surface. The average activation energy for each site type cannot be calculated during the simulations using Eq. (37) but, rather, a variation of Eq. (16) applied to the different subtypes within the same site type. As we will see in realistic simulations of wet chemical etching (Sec. VI), surface atoms belonging to the same site-type α (i.e., sharing the same prefactor $p_{0\alpha}$) can have very different activation energies, depending on the local coverage by H and OH groups, thus forming discrete sets of energies. In that case, Eq. (37) will not provide the average activation energy of the atom type considered.

Figure 6(c) shows that the average surface fractions $\langle f_\alpha \rangle$ in the one-dimensional interface model are not described by Eq. (29) ($\langle f_\alpha \rangle_{\text{master}}$ in the figure). The disagreement is not due to numerical error and similar results are obtained for cases E, F, and H. The reason for the failure of Eq. (29) in the current model lies in the fact that the transition matrix is determined by the removal probabilities (and the underlying geometry), so that it is not an independent parameter as it is implicitly assumed in the analytical derivation of Sec. IV B. A physically more meaningful argument is that in the TFC model, for every particle that is removed, a new replacing particle appears, but, in the current model, the removal of one particle may be followed by the incorporation of two particles or no particles at all. Besides, in the current model

there exists a nonlinear effect associated to the update of the atom type of the neighboring sites, which is not present in the TFC model.

Finally, Fig. 7(b) shows the relative contributions ϵ_α of each atom type to the total macroscopic activation energy for cases E-H and compares them to the normalized fractions of removed particles $\langle w_\alpha^\uparrow \rangle$. This shows that the weights $\langle w_\alpha^\uparrow \rangle$ can be used during a simulation as indicators of the relative importance of the different site types, even if the actual values of $E_{\langle f_\alpha \rangle}$ and $E_{\langle p_\alpha \rangle}$ (required to evaluate ϵ_α) are not known.

The results of this section show that, also for the one-dimensional interface system, the (temperature-averaged) macroscopic activation energy can be approximated by evaluating the term $E_a^{(f)}$ *a posteriori* from the temperature dependence of the surface fractions $\langle f_\alpha \rangle$. Even though the explicit expression for the temperature dependence of $\langle f_\alpha \rangle$ is not known and the value of the activation energy cannot be calculated at each temperature during a simulation, the weights $\langle w_\alpha^\uparrow \rangle$ can be used to identify the relative importance of the different sites.

VI. ANISOTROPIC WET CHEMICAL ETCHING OF SILICON

A. Realistic model

Anisotropic wet chemical etching is a nonequilibrium process in which both the microscopic roughness and morphology, and the macroscopic orientation-dependent etch rate are determined by the relative values of the microscopic (atomistic) reaction rates. Gosálvez *et al.* [13] have shown that the origin of the (large) differences in site-specific rates is found in two microscopic mechanisms: the weakening of backbonds following OH termination of surface atoms and the existence of significant interaction between the terminating species (H/OH). The weakening of the backbonds depends only on the *total number* of hydroxyls attached to the two atoms sharing the bond and is independent of the particular distribution of the OH groups between the two atoms [13], in such a way that each backbond is weakened by the same energy $\epsilon \approx 0.4$ eV for every OH group that is attached to either atom. Thus, the energy of a bond between an atom terminated by i OH groups and an atom terminated by j groups ($i,j = 0,1,2,3$) can be written as

$$\epsilon_{ij} = \epsilon_0 - (i+j)\epsilon, \tag{38}$$

where ϵ_o is the bond energy between two bulk atoms ($\epsilon_0 \approx 2.7$ eV). Correspondingly, the total bonding energy for a surface atom with n first neighbors is simply the sum of the energies of the n bonds:

$$E_{\text{bonds}} = \sum_{j=1}^{n} \epsilon_{m,m_j}, \tag{39}$$

where we have considered the most general case, in which the target atom is terminated by m OH groups ($m \leq 4-n$)

and the jth first neighbor ($j=1,2,\ldots,n$), having itself n_j first neighbors, is terminated by m_j OH groups ($m_j \leqslant 4 - n_j$).

The other microscopic mechanism of major importance in wet chemical etching, namely, the interaction between the surface terminating groups (H/OH), occurs only in the presence of *indirect second neighbors* [14,15]. Due to these interactions, hydroxyl termination of the target atom (and its first neighbors) involves additional energy terms, not taken into account in Eq. (39). As a result, the total (local) energy of a surface atom can be expressed as the sum of three terms [14]:

$$E = E_{\text{bonds}} + \sum (e^{TA}_{\text{OH/H}} + e^{TA}_{\text{OH/OH}}) + \sum (e^{FN}_{\text{OH/H}} + e^{FN}_{\text{OH/OH}}),$$

(40)

where E_{bonds} is the energy of Eq. (39) and $\Sigma(e^{TA}_{\text{OH/H}} + e^{TA}_{\text{OH/OH}})$ [$\Sigma(e^{FN}_{\text{OH/H}} + e^{FN}_{\text{OH/OH}})$] symbolically denotes the total energy from the interactions between the OH groups terminating the target atom (TA) [the first neighbors (FN)] and H and/or OH terminating the indirect second neighbors of the TA (FN). The geometrical restrictions to hydroxyl termination in the presence of indirect second neighbors is a manifestation of the important role of steric hindrance in anisotropic wet chemical etching. In the present model, the source of steric hindrance is identified as the (H/OH-terminated) indirect second neighbors.

Note that, although the parameters ϵ and ϵ_0 used for describing the bonding energy are fixed by the first-principles *ab initio* study [13], the interaction energies $e^{TA,FN}_{\text{OH/OH}}$ and $e^{TA,FN}_{\text{OH/H}}$ can be used as tunable parameters in order to describe different etchants. Once an etchant is chosen, its concentration is described in the model by the amount of surface coverage by OH groups.

As with the previous simpler models for wet chemical etching, the local dynamics of this model consists of random removals of surface sites with probabilities

$$p = p_0 e^{-\Delta E/k_B T},$$

(41)

where the activation energy ΔE is defined as

$$\Delta E = \max(0, E - E_c).$$

(42)

Here, p_0 and E_c are parameters describing the different surface atom types (as $p_{0\alpha}$ and E_α previously). We have dropped the index α to stress the fact that the local energy E is calculated using the same expression [Eq. (40)] for all site types. The use of the function $\max(0, E - E_c)$ mimics the Metropolis algorithm [16]. Following the discussion of Gosálvez *et al.* in Ref. [14], and the notation used in surface studies of Si(111) [17], we consider the following surface site types.

(1) Type 0: Nonbonded atoms that have not been removed, *unlinked*.

(2) Type 1: Singly bonded atoms: *trihydrides*; also referred to as *kinks*.

(3) Type 2A: Two-bonded atoms on ideal (100) surfaces, *terrace dihydrides*.

(4) Type 2B: Vertical two-bonded atoms at ideal $[\bar{1}2\bar{1}]$ steps, *vertical step dihydrides*.

(5) Type 2C: Horizontal two-bonded atoms at ideal $[\bar{1}2\bar{1}]$ steps, *horizontal step dihydrides*; plus all other possible two-bonded atoms.

(6) Type 3A: Three-bonded atoms at ideal (111) surfaces, *terrace monohydrides*.

(7) Type 3B: Three-bonded atoms at ideal $[1\bar{2}1]$ steps, *step monohydrides*; plus all other possible three-bonded atoms.

Note that the atoms of type 0 are included for completeness since they can occasionally appear in connection with the formation of overhangs. This is, however, a rare event in the simulations and has no measurable effect on the evolution of the surface. These atoms are removed (with probability 1) as soon as they are encountered and, accordingly, we can say that in this model the surface contains $M = 6(+1)$ types of atoms.

The six pairs of parameters (p_0, E_c) for Types $1, 2A, \ldots, 3B$ can be determined from comparison to experiment. The idea is to choose the parameters so that the relative values of the etch rates of a number of surface orientations (six, in principle) agree with those from an experiment. By adjusting the parameters p_0, the simulated etch rates will shift up/down in an Arrhenius plot. Similarly the slopes of the etch rates can be controlled by tuning the parameters E_c. Alternatively, it is also possible to choose the parameters (p_0, E_c) based on comparison of the simulated surface morphology with that from experiments. An example of this approach is provided in Ref. [2].

Note that due to the different possible combinations of the terminating species H and OH around a surface site, the activation energies ΔE take different values for atoms of the same type. This situation resembles that of case G for the one-dimensional interface in Sec. V, where the activation energy of each atom type was randomly chosen from a uniform distribution in an energy interval. However, in the current case the distribution is not uniform, but rather, a discrete set of activation energies. Thus, the problem of determining the average activation energy for an atom type is formally equivalent to the problem of determining the macroscopic activation energy for the whole surface and Eq. (37) should not be expected to be valid.

B. Results for the realistic model

In this section, we report on the relation between macroscopic and microscopic activation energies for the two surface orientations of silicon with highest technological interest: Si(100) and Si(110).

The parameters of the model [$e^{TA,FN}_{\text{OH/OH}}$, $e^{TA,FN}_{\text{OH/H}}$, (p_0, E_c) and θ] are chosen to simultaneously provide the formation of pyramidal hillocks on Si(100) and nosed-zigzag structures on vicinal Si(110), as shown in Ref. [2]. In the case of Si(100), we consider the fully texturized steady-state surface, completely covered with pyramids [2].

Figure 8(a) shows the etch rate of the two surface orientations considered, both as the rate of removal of particles $\langle \dot{f}^{\uparrow} \rangle$ and as the actual etch rate R. The similarity between the
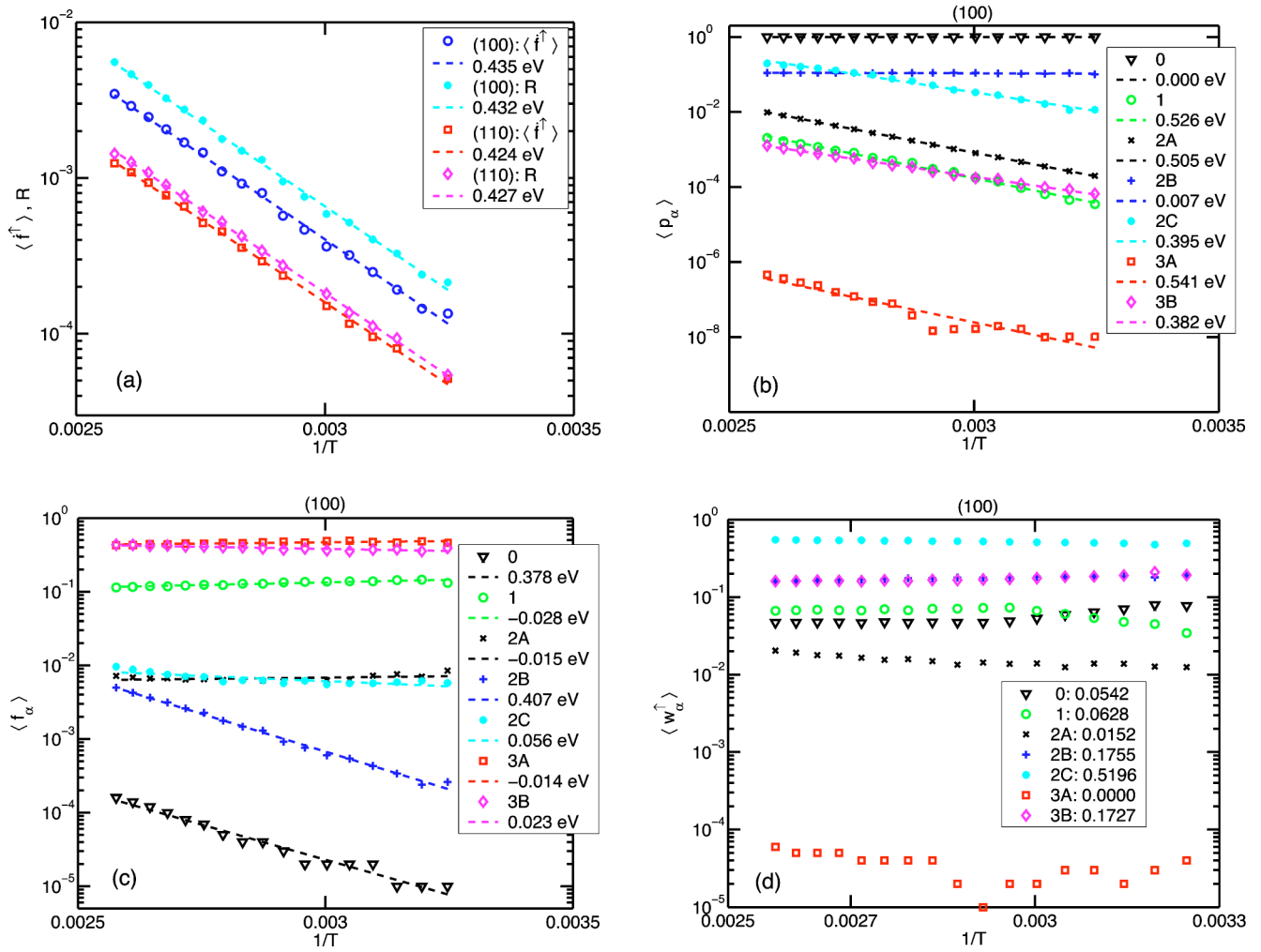
FIG. 8. (Color online) (a) Etch rate R and rate of removal of particles $\langle \dot{f}^{\uparrow} \rangle$ for (100) and (110). (b),(c) Determination of the activation energies $E_{\langle p_\alpha \rangle}$ and $E_{\langle f_\alpha \rangle}$ ($\alpha = 0,1,2A,\ldots,3B$) for (100). (d) Temperature dependence of the normalized fractions of removed particles $\langle w_\alpha^{\uparrow} \rangle$.
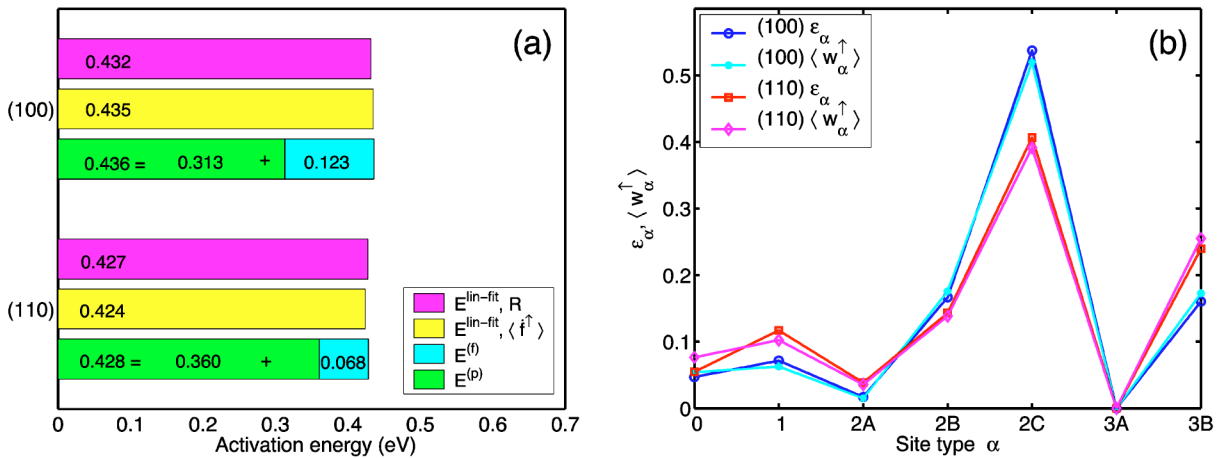

FIG. 9. (Color online) (a) Activation energy $E_a^{\text{lin-fit}}$ explained as the sum $E_a^{(p)} + E_a^{(f)}$ [Eq. (16)] for Si(100) and Si(110). (b) Relative contributions ϵ_α [Eq. (18)] compared to the normalized fractions $\langle w_\alpha^{\uparrow} \rangle$ [Eq. (15)] for Si(100) and Si(110). Straight lines are guides for the eyes.

activation energies demonstrates that R is proportional to $\langle \dot{f}^{\uparrow} \rangle$, as claimed in Sec. III A. In order to understand the origin of the macroscopic activation energy for Si(100) in this fully texturized regime, the *a posteriori* analysis of the temperature dependence of the removal probabilities $\langle p_\alpha \rangle$ and the surface fractions $\langle f_\alpha \rangle$ is provided in Figs. 8(b) and 8(c). The activation energies $E_{\langle p_\alpha \rangle}$ and $E_{\langle f_\alpha \rangle}$ are obtained as the slopes of the linear fits. Figure 8(d) shows the temperature dependence of the weights $\langle w_\alpha^{\uparrow} \rangle$, illustrating that, even though the removal probabilities and the surface fractions may vary strongly, the normalized fraction of removed particles is comparatively a rather smooth function of temperature. Taking the average values of $\langle w_\alpha^{\uparrow} \rangle$ over all temperatures [legend of Fig. 8(d)] and using them in Eq. (16) together with the values determined for $E_{\langle p_\alpha \rangle}$ and $E_{\langle f_\alpha \rangle}$ show [Fig. 9(a)] that the macroscopic activation energy is described as the sum of the two terms $E_a^{(p)} + E_a^{(f)}$ [Eq. (16)]. This figure shows that also the macroscopic activation energy of Si(110) can be described as the sum of these two terms.

Finally, we show the relative contributions ϵ_α of each atom type to the total macroscopic activation energy in Fig. 9(b) and compare them to the normalized fractions of removed particles $\langle w_\alpha^{\uparrow} \rangle$. According to this figure, the etching process under the chosen conditions is dominated by the same surface sites in these two surface orientations: horizontal step dihydrides ($2C$), step monohydrides ($3B$) and vertical step dihydrides ($2B$). The fact that the contribution from 3B is larger in (110) than in (100) stems from the fact that the step monohydrides are the natural termination of (110) (100% in the ideal surface and about 60% in these simulations) while in (100) they appear mostly at pyramidal ridges and at the steps between the (111)-terraces forming the pyramidal facets [2] [about 40% in these simulations, cf. Fig. 8(c)]. Although the presence of the horizontal step dihydrides ($2C$) on these orientations is only a small fraction (below 1%) in both surfaces, as shown in Fig. 8(c) for (100), their relatively high removal probability [Fig. 8(b)] makes them dominate the etching process. The same applies to the vertical step dihydrides ($2B$), which are present on surface by a fraction of a percent, as shown in Fig. 8(c) for (100). These results show quantitatively that the minority species do control the etching process and that usually the macroscopic activation energy cannot be attributed to only one single species, not especially to the majority species, as is extended practice in wet chemical etching. We conclude that the weights $\langle w_\alpha^{\uparrow} \rangle$ can be used during a simulation as indicators of the relative importance of the different site-types, even if the actual values of $E_{\langle f_\alpha \rangle}$ and $E_{\langle p_\alpha \rangle}$ (required to evaluate ϵ_α) are not known.

The previous discussion allows us to conclude that, in the fully pyramid-covered regime of Si(100), the microscopic mechanisms controlling the etching process are the same as in Si(110), even if these two surface orientations display very different morphologies, as shown in Ref. [2]. This conclusion

should not be understood as a general proof that equal macroscopic activation energies imply the same microscopic processes. The present work shows that the macroscopic activation energy is a very complicated quantity that cannot be identified with only one atomistic process and that, in principle, similar numerical values can be obtained for it with different combinations of weights for different processes.

VII. CONCLUSIONS

By using the case of anisotropic wet chemical etching as a particular example of nonequilibrium systems with open moving surfaces, it is shown that the macroscopic activation energy E_a (defined as the slope of the etch rate in an Arrhenius plot) is explained by the sum of two terms $E_a^{(p)} + E_a^{(f)}$. The first term $E_a^{(p)}$—sometimes wrongly identified as the activation energy itself—corresponds to the average of the microscopic activation energies $E_{\langle p_\alpha \rangle}$, and the additional term $E_a^{(f)}$ accounts for the existence of fluctuations in the fractions of particles f_α at fixed temperature. This shows that the description of the macroscopic activation energy as a "total surface energy," such as $\Sigma_\alpha \langle f_\alpha \rangle E_{\langle p_\alpha \rangle}$, is not valid for these systems and will lead to erroneous interpretations of results. As a matter of fact, the "total energy" concept is shown to be correct only in the particular case that the transition matrix ($\pi_{\alpha\beta}$) does not depend on temperature, which is not the case in realistic models of growth and etching. In these models, ($\pi_{\alpha\beta}$) is a complex function of the removal probabilities, of the temperature, and of the geometrical structure of the material, as shown by the particular examples considered for chemical etching in this study.

It is shown that the correction term $E_a^{(f)}$ can be accurately determined by *a posteriori* analysis of the temperature dependence of the surface fractions in all cases considered. A model is presented in which this term can be calculated analytically. Further work would be needed if the corresponding analytical expression for the more realistic models is desired.

It is also shown that the normalized fractions of removed particles $\langle w_\alpha^{\uparrow} \rangle$ can be used as indicators of the relative importance of the different surface sites for the growth/etch process. This enables a quantitative measure of the way how the minority species dominate the process and stresses the fact that the macroscopic activation energy is a complicated function and should not be identified with one atomistic process only; especially not with the majority species on surface, as seems to be extended practice in growth and etching.

[1] J. Flidr, Y.C. Huang, T.A. Newton, and M.A. Hines, J. Chem. Phys. **108**, 5542 (1998).

[2] M.A. Gosálvez and R.M. Nieminen, New J. Phys. **5**, 100 (2003).

[3] L.D. Landau and E.M. Lifshitz, *Statistical Physics*, 3rd ed. (Pergamon Press, Oxford, 1989), Pt. 1.

[4] H. Seidel, L. Csepregui, A. Heuberger, and H. Baumgärtel, J. Electrochem. Soc. **137**, 3612 (1990).

[5] M. Shikida, K. Sato, K. Tokoro, and D. Uchikawa, Sens. Actuators **80**, 179 (2000).

[6] M.A. Gosálvez, R.M. Nieminen, P. Kilpinen, E. Haimi, and V. Lindroos, Appl. Surf. Sci. **178**, 7 (2001).

[7] R.A. Wind, H. Jones, M.J. Little, and M. Hines, J. Phys. Chem. B **106**, 1557 (2002).

[8] N. Goldenfeld, *Lectures on Phase Transitions and the Renormalization Group* (Addison-Wesley, Reading, MA, 1996).

[9] F.Y. Wu, Rev. Mod. Phys. **54**, 235 (1982).

[10] A. Papoulis, *Probability, Random Variables and Stochastic Processes* (McGraw-Hill, New York, 1965), pp. 533–535.

[11] For equal activation energies ($E_1 = E_0 = E$), the macroscopic activation energy trivially takes the only possible value E.

[12] S.T. Bramwell, P.C.W. Holdsworth, and J.F. Pinton, Nature (London) **396**, 552 (1998).

[13] M.A. Gosálvez, A.S. Foster, and R.M. Nieminen, Europhys. Lett. **60**, 467 (2002).

[14] M.A. Gosálvez, A.S. Foster, and R.M. Nieminen, Appl. Surf. Sci. **202**, 160 (2002).

[15] M.A. Gosálvez, A.S. Foster, and R.M. Nieminen, Sens. Mater. **15**, 53 (2003).

[16] N. Metropolis, A.W. Rosenbluth, M.N. Rosenbluth, A.H. Teller, and E. Teller, J. Chem. Phys. **21**, 1087 (1953).

[17] J. Kasparian, M. Elwenspoek, and P. Allongue, Surf. Sci. **388**, 50 (1997).